Journal of Engineering, Project, and Production Management
2022, 12(3), 259-268

Intelligent Control and Parameter Calculation of Highway Truck Escape Ramp

Xinghua Hu[1], Hongbin Qin[2], Yaqi Zhu[3], Wei Liu[4], and Gao Dai[5]
[1]Professor, School of Traffic & Transportation, Chongqing Jiaotong University, Chongqing, China, E-mail: xhhoo@cqjtu.edu.cn (corresponding author).
[2]Graduate Student, School of Traffic & Transportation, Chongqing Jiaotong University, Chongqing, China, E-mail: 622190950010@mails.cqjtu.edu.cn
[3]Graduate Student, College of Transportation Engineering, Chang'an University, Xi'an, China, E-mail: zyq95427@qq.com
[4]Professor, School of Traffic & Transportation, Chongqing Jiaotong University, Chongqing, China, Email: neway119@qq.com
[5]Senior Engineer, Chongqing Ulit Science & Technology Co., Ltd, Chongqing, China, Email: 1090685519@qq.com

Engineering Management
Received December 14, 2021; revised May 7, 2022; accepted June 19, 2022
Available online July 26, 2022

Abstract: To reduce the probability of secondary accidents caused by the direction deviation, body rollover, and excessive deceleration of runaway vehicles during braking on a truck escape ramp (TER), the safety of the occupants and the vehicles must be ensured. Based on the momentum theorem, an intelligent control method for a TER is proposed. In the method, a slope aggregate with a small rolling resistance coefficient is used on the original escape lane, and the information acquisition, braking device control, and braking modules are established. Through these modules, the operation parameters and control parameters of the out-of-control vehicle are obtained in advance, to control the operation state of the runaway vehicle. Achieve the purpose of reducing the braking effect of the slope bed aggregate and ensuring maximum utilization of the braking ramp. Finally, the proposed control method is simulated on the MATLAB/Simulink simulation platform. The results show that the control method can realize safe braking of an out-of-control vehicle at various speeds and different mass conditions, and it can play a highly significant role in the braking of high-speed and heavy-duty vehicles.

Keywords: Truck escape ramp, momentum theorem, whole vehicle body function, intelligent control process, control parameter.

DOI 10.32738/JEPPM-2022-0024

1. Introduction

In recent years, the highway construction in China has developed rapidly, and by the end of 2020, the highway lane mileage was 723,100 kilometers. Restricted by the topography, the downhill sections of expressways are commonly long and steep, which frequently have a high incidence of road traffic accidents. The establishment of truck escape ramps (TERs) is currently one of the most effective engineering measures to solve the traffic safety problem of such sections (Greto and Easa, 2019). A TER refers to a dedicated lane added outside the carriageway of a long steep downhill road for vehicles with out-of-control speeds (brake failure) to leave the main line for safe deceleration. It is composed of an approach road, a brake lane, a service lane, and other ancillary facilities (Wang and Zhang, 2012).

The research on TERs has mainly focused on the basis for setting a TER and its components. Regarding the former, the American Society of Civil Engineers introduced a method to determine whether it is necessary to establish an escape lane (Hancock and Wright, 2013). Al-Madani and Al-Janahi (2012) summarized the influencing factors of TERs settings. Wu (2006) proposed a design method for TERs. Each part of an escape lane plays a crucial role in the safe braking of vehicles. Song and Guo (2016) proposed a setting method for service lanes by analyzing the driving stability and direction adjustment times of out-of-control vehicles. Then they proposed the design parameters of the width of TERs and the length of approach roads based on the UC-Win/Road Ver. 9 driving simulation platform (Song and Guo, 2017; Song and Guo, 2016). Regarding the setting of auxiliary facilities, Mi et al. (2020) studied the setting modes of traffic safety facilities, such as traffic signs and markings of TERs. Although there have been many studies on the setting of TERs, escape lanes have been established based on the relevant specifications of highway constructions. However, the phenomena of secondary

damage to vehicles entering TERs are widespread. The common problems in TERs mainly include the following: when the speed of an out-of-control vehicle is extremely high, it cannot stop completely, and a part of the body still rushes out of the TER; the ramp aggregate causes a runaway vehicle to significantly decelerate; therefore, the external force is extremely large in a short time, resulting in secondary injuries; the rapid steering or the change in the road conditions cause the vehicle body to deviate or even roll over during braking.

In view of the above problems, design concepts have been proposed based on existing TERs. Capuano et al. (2018) proposed a novel escape lane braking system, which was mainly formed of deformable cement-based materials and can produce uniform resistance when in contact with vehicle tires. Nishiyama (2017) and Michael (2015) analyzed the driving process of vehicle tires in the braking ramp and studied the tire stress of the vehicle during the braking process. Qin et al. (2021) optimized the flexible protective net installed at the end of a TER, including its overall size, material, and shape. Yan et al. (2015) proposed a net energy absorption system for a TER to compensate for its short length. Although the above research can compensate for the deficiencies of TERs to some extent, there are few studies on predicting or controlling the driving state of runaway vehicles on TERs. Owing to the uncontrollability of runaway vehicles when decelerating on an escape lane, secondary accidents, such as direction deviation, rollover, and retrogression, may still occur.

Considering the above background, this paper proposes an intelligent control method for a TER. The control method predicts the driving state of a runaway vehicle on a TER by combining the momentum theorem with information technology. Moreover, it realizes the control of the braking process by setting a braking device to ensure that the runaway vehicle maximizes the use of the braking lane length. This reduces the external force in the process of vehicle deceleration and decreases the probability of secondary accidents of runaway vehicles.

2. Concept of Escape Lane Control Based on Momentum Theorem

2.1. Momentum Theorem

According to the momentum theorem, the difference in the momenta of an object at the beginning and end of a process is equal to the impulse of the force acting on it in the process, i.e., the product of the force and the action time of the force (Haugland, 2013). The calculation formula is expressed in Eq. (1).

$$Ft = m(V_0 - V_1) \tag{1}$$

where F — the external force on the object, t — action time of the external force in s, m — the object mass in kg, V_0— the initial velocity of the object in m/s, and V_1 — the velocity of the object at the end of time t in m/s.

2.2. Application of Momentum Theorem to Escape Lane

The time change rate of the momentum of a vehicle directly reflects the impulse experienced by the vehicle body, and therefore, determines the degree of the secondary damage to the vehicle body and the occupants. For a runaway vehicle, the speed change is the initial value of the speed before entering the TER. Therefore, to realize minimum force on a vehicle in the deceleration process on a TER, it is necessary to extend the action time of the external force to the maximum extent. There is a direct relationship between the braking time and the braking distance, which is expressed in Eq. (2).

$$L=\frac{1}{2}at^2 \tag{2}$$

where L — the braking distance in m, and a — the braking deceleration in m/s^2, where $a=\frac{F}{m}$.

By combining Eq. (1) and (2), the relationship between the external force and the braking distance can be expressed as Eq. (3).

$$F=\frac{mV_0^2}{2L} \tag{3}$$

Therefore, if the external force on a vehicle is to be minimized, the braking distance should be extended to the maximum extent. In the setting of the length of the braking ramp of a TER, effective use of the maximum braking distance should be ensured. In addition, based on Eq. (3), the external force on a vehicle during deceleration can be determined from the effective braking distance, initial vehicle speed, and total vehicle weight.

Based on the above, the main concept of the intelligent control method for a TER proposed in this paper is to use a slope aggregate with a small rolling resistance coefficient in the original avoidance lane and add information acquisition devices, braking control devices, and braking devices. Pre-collected the parameters of the escape lane and the runaway vehicle, including the length of the approach road, gradient, and maximum length of the braking ramp, as well as the contour, speed, and weight of the runaway vehicle. Using these parameters, the best braking force of the vehicle in the braking process is calculated, and vehicle braking control is realized with the aid of a braking device. This method enables the runaway vehicle to maximize the use of the braking ramp of the TER to complete braking under the premise of ensuring safety and reducing the effect of the external force. This consequently reduces the degree of secondary injury to the vehicle and its occupants.

3. Intelligent Control Method of TER

3.1. Overall Framework

The intelligent control system for a TER mainly comprises three parts: the information acquisition module, braking device control module, and braking module. Its schematic is shown in Fig. 1.

3.2. Function Realization

The information acquisition module is located in the approach area, which is mainly composed of a radar speedometer, a lidar, and radio frequency identification (RFID) equipment. It is used to collect the vehicle speed, total weight, and contour and transmit these parameters to the braking device control module. The control module of the braking device mainly calculates the data needed for braking an out-of-control vehicle, and it adaptively adjusts the braking device.

(1) Speed acquisition method

A radar is commonly used for the estimation of vehicle speed, distance, and direction (Patole et al., 2017).

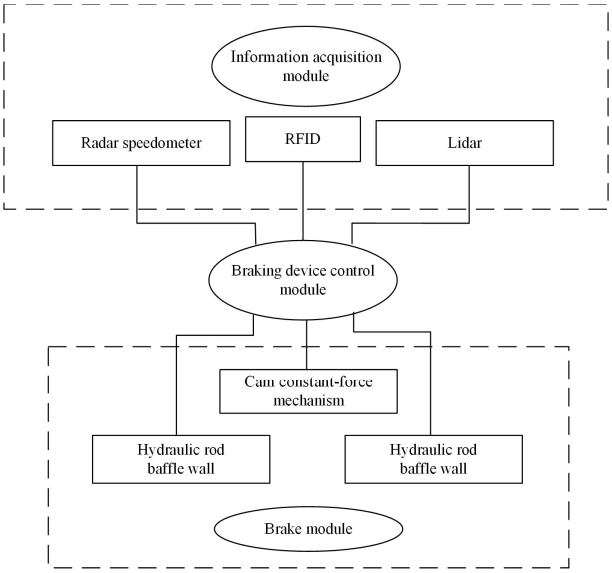

Fig. 1. Composition of the intelligent control system for avoidance lane

The basic principle of vehicle speed estimation is using the Doppler effect of the reflected waves. When a vehicle approaches a radar, the microwaves emitted by the radar are reflected by the vehicle. The vehicle speed is measured based on its relationship with the frequency difference of the emitted and reflected waves (Shariff et al., 2017). For the speed measurement of a runaway vehicle, before it enters a TER, the narrow-beam radar can effectively avoid the speed interference of vehicles in adjacent lanes and has more advantageous than ordinary speed radars.

(2) Vehicle mass collection method

RFID technology can identify specific targets and read messages through wireless signals (Pawłowicz et al., 2020). The principle of RFID-based vehicle identification technology is as follows. The electronic license plate (radio frequency tag) is installed on the windshield of the vehicle, and a series of information related to the motor vehicle is associated with the electronic license plate, including the unique identification number and type of the vehicle, etc. When an out-of-control vehicle with an RFID electronic license plate passes a collector, the collector will identify information of the corresponding electronic license plate. Moreover, the electronic license plate is matched to the weighing data of the toll station at the entrance of the expressway, therefore, the quality of the vehicle can be collected through the electronic license plate.

(3) Vehicle contour data acquisition method

At present, vehicle automatic measurement equipment is mainly based on machine vision, infrared curtains, and lidar technology. Compared with machine vision and infrared curtains, lidar has the characteristics of high data accuracy, high scanning speed, and a large sensing range (Zhao et al., 2019), which can better meet the needs of vehicle contour measurement than the other methods.

(4) Braking control method

The brake device mainly includes a baffle wall, hydraulic rod, and can constant-force mechanism. Its schematic is shown in Fig. 2.

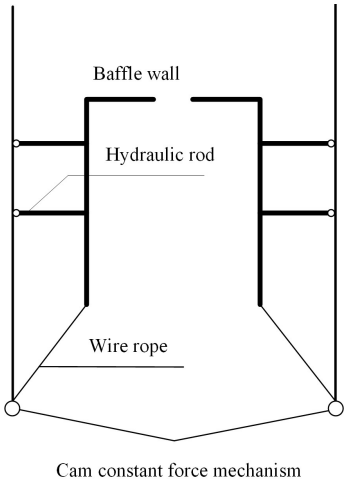

Fig. 2. Schematic of the braking device

The baffle wall is L right-angled, and its contact surface with a car has an energy-absorbing layer. The front part of the baffle wall can block the front impact of the vehicle, and the side part has a side effect on the car body under the action of the hydraulic rod to ensure the stability of the direction of the out-of-control vehicle. The hydraulic rod is sliding connected with the braking lane to push the baffle wall to move longitudinally and transversely. The cam constant-force mechanism is connected with the baffle wall by a steel cable, which applies a backward pulling force on the baffle wall along the slope surface, and is an important device that offers additional vehicle resistance during the entire braking process. The plan view of the main installations in a TER is shown in Fig. 3.

4. Calculation of Intelligent Control Parameters for TER

In this study, the entire process from a vehicle entering the approach road to the final braking is divided into three stages. The first stage is the stage of the runaway vehicle driving on the approach road. The second stage is the braking stage of the out-of-control vehicle on the ramp bed alone. The third stage is the braking stage in which the vehicle and the baffle wall move together.

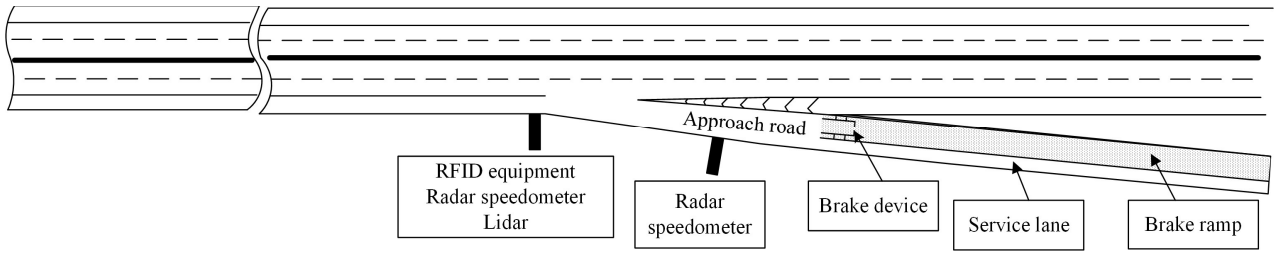

Fig. 3. Plan view of main installations in TER

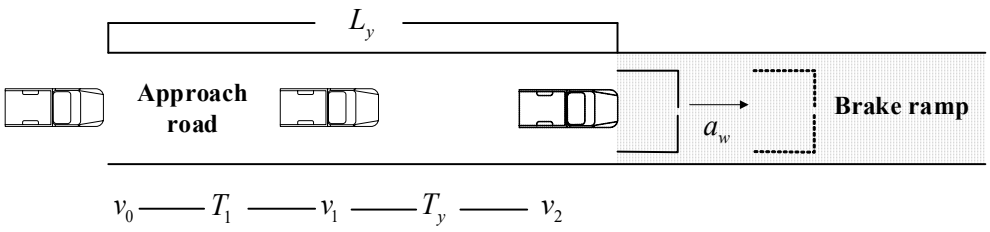

Fig. 4. Schematic of approach road driving stage

4.1. Analysis of Vehicle Running on Approach Road

When a runaway vehicle enters the approach road, it starts to decelerate, and the speed of the vehicle at the entrance of the approach road is recorded as v_0. When the radar detects that the runaway vehicle has reached the middle section of the approach road, the hydraulic rod and the baffle wall together start to move along the brake ramp with acceleration a_w. The running speed of the out-of-control vehicle collected in the middle section of the approach road is denoted as v_1, and the time interval between v_0 and v_1 is denoted as T_1. The schematic diagram is shown in Fig. 4.

The deceleration, a_y, of the vehicle in T_1 period is expressed as Eq. (4).

$$a_y = \frac{v_0 - v_1}{T_1} \tag{4}$$

Assuming that the runaway vehicle maintains a deceleration of a_y and drives on the second half of the approach road, the total length of the approach road is denoted as L_y. Thus, speed v_2 and driving time T_y when the vehicle reaches the braking slope bed are as expressed in Eq. (5) and (6), respectively.

$$v_2 = \sqrt{v_0^2 - 2a_y L_y} \tag{5}$$

$$T_y = \frac{v_1 - v_2}{v_0 - v_1} T_1 \tag{6}$$

4.2. Analysis of Vehicle Operation and Calculation of Control Parameters in Braking Stage of Slope Bed

After a runaway vehicle enters the braking lane, it decelerates on the braking slope bed, and the hydraulic rod and the baffle wall together continue to move along the braking slope bed with acceleration a_w. Until the end of time t_1, the speed of the baffle wall is equal to the speed of the out-of-control vehicle, and the speed is denoted as v_3. At this time, the baffle stops working, and the front end and side part of the baffle fits with the vehicle body under the action of the hydraulic rod, assuming that there is no interaction between them. This stage mainly calculates vehicle operating parameter v_3 and control parameter a_w. The schematic diagram is shown in Fig. 5.

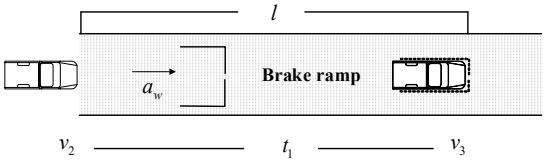

Fig. 5. Schematic of slope bed braking stage

During the deceleration process of the vehicle on the brake ramp, the forces experienced by it mainly include the vehicle driving force, vehicle braking force, air resistance, rolling resistance between the vehicle tires and the road surface, gradient resistance, and other forces.

(1) Vehicle driving force

From investigations and research, it is found that the vehicles entering a TER are generally classified into two types. In one case, the driver does not control the vehicle speed appropriately in the long continuous downhill section, which leads to a high vehicle speed and the risk of becoming out of control. Therefore, it is urgent to enter a TER to slow down and avoid danger. In the second case, mechanical failure or frequent braking deceleration of a running vehicle for a long time leads to braking failure. Regardless of the above scenarios, for traffic safety and vehicle operation needs, the driver will turn off the engine before entering a TER, so that the vehicle loses the driving force and slide forward. Therefore, the driving force of the vehicle is zero in the parameter calculation.

(2) Vehicle braking force

When a car is braking, it applies a braking force to the wheel to prevent the wheel from moving forward. The maximum value depends on the adhesion between the tire and the road. If the braking force of a vehicle is greater than the adhesion force when driving on the road, the wheels will stop rotating, and the driving stability will be affected. Considering that vehicles using an escape lane completely lose their braking ability before entering a TER, based on the most unfavorable scenario—vehicles entering an escape lane lose their braking force, and the braking force is zero.

(3) Air resistance

Based on aerodynamics studies, the direction of air resistance is parallel to the braking ramp and opposite to the driving direction during the driving of a vehicle, and its magnitude is proportional to the relative speed of the vehicle and the air. The expression of air resistance is shown in Eq. (7) (Bauskar et al., 2019).

$$F_a = \frac{1}{2} K A_1 \rho V^2 \tag{7}$$

where K — the coefficient of air resistance, A_1 — the windward area of the vehicle in m^2, ρ — the air density in $N \cdot s^2/m^4$, and V — the relative speed of the vehicle to the air, which is approximately the running speed of the vehicle in m/s.

When the speed of a runaway vehicle changes from v_2 to v_3, air resistance F_{a1} is expressed in Eq. (8).

$$F_{a1} = \frac{\int_{v_3}^{v_2} \frac{K A_1 \rho V^2}{2} dv}{v_2 - v_3} \tag{8}$$

(4) Rolling resistance

The rolling resistance direction is parallel to the braking ramp, which hinders the driving speed of the vehicle. Its magnitude is related to the total vehicle weight, lane slope, and rolling resistance coefficient between the tires and the road surface. Rolling resistance $F_{\Gamma 1}$ is expressed in Eq. (9).

$$F_{\Gamma 1}=mg\cos\alpha D_f \tag{9}$$

where D_f — the rolling resistance coefficient of the aggregate on the braking ramp, m — the total weight of the runaway vehicle in kg, g — the acceleration of gravity in m/s^2 and a — the brake ramp angle.

(5) Ramp resistance

Ramp resistance F_{g1} is as expressed in Eq. (10).

$$F_{g1}=mg\sin\alpha \tag{10}$$

The force diagram of a vehicle on a braking ramp is shown in Fig. 6.

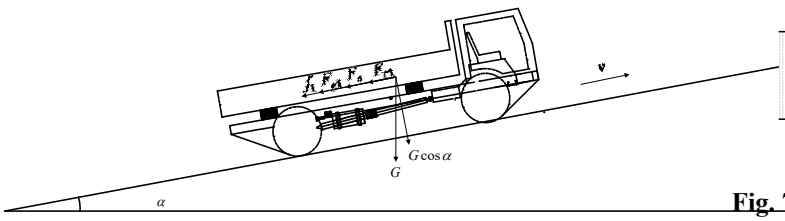

Fig. 6. Force diagram of a vehicle on a braking ramp

The process of an out-of-control vehicle slowing down on a brake ramp until it touches the baffle wall follows the law of conservation of energy. The calculation formula is expressed in Eq. (11) (Raslavičius, et al., 2017).

$$\frac{1}{2}mv_2^2-\frac{1}{2}mv_3^2=(F_{\Gamma 1}+F_{a1}+F_{g1})l+W_{f1} \tag{11}$$

where v_2 — the initial speed of the runaway vehicle entering the brake bed in m/s, v_3 — the speed when the out-of-control vehicle and the baffle wall are relatively stationary in m/s, m — the total weight of the runaway vehicle in kg, l — the distance of the runaway vehicle driving on the brake bed in m, and W_{fl} — the total work done by other forces.

The running distance, l, of a runaway vehicle on the braking slope bed of a TER is the running distance of the baffle wall in time $T_y + t_1$, which is expressed in Eq. (12).

$$l=\frac{1}{2}a_w\left(T_y+t_1\right)^2 \tag{12}$$

v_3 is the velocity of the baffle wall at the end of time $T_y + t_1$, which is expressed in Eq. (13).

$$v_3=a_w\left(T_y+t_1\right) \tag{13}$$

By combining Eq. (11), (12), and (13), a_w and v_3 can be obtained as expressed in Eq. (14) and (15), respectively.

$$a_w=\frac{\sqrt{\left(F_{\Gamma 1}+F_{a1}+F_{g1}\right)^2\left(T_y+t_1\right)^2-4mW_{f1}+4m^2v_2^2}}{2m\left(T_y+t_1\right)}-\frac{F_{\Gamma 1}+F_{a1}+F_{g1}}{2m} \tag{14}$$

$$v_3=\frac{\sqrt{\left(F_{\Gamma 1}+F_{a1}+F_{g1}\right)^2\left(T_y+t_1\right)^2-4mW_{f1}+4m^2v_2^2}}{2m}-\frac{\left(F_{\Gamma 1}+F_{a1}+F_{g1}\right)\left(T_y+t_1\right)}{2m} \tag{15}$$

4.3. Calculation of Control Parameters of Vehicle and Baffle Wall as Complete Deceleration Stage

After the baffle wall is fitted to the car body, the baffle wall, hydraulic rod, and runaway vehicle begin to decelerate together at speed v_4 and will complete the braking under the pulling force, T, provided by the cam constant-force mechanism. T is the control parameter to be calculated in this stage. The schematic diagram is shown in Fig. 7.

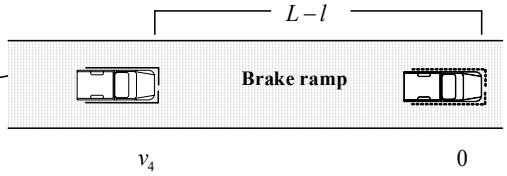

Fig. 7. Vehicle and baffle wall in complete deceleration stage

The moment when the speed of the runaway vehicle changes from v_3 to v_4 follows the law of conservation of momentum. The calculation formula is expressed in Eq. (16).

$$mv_3=(M+m)v_4 \tag{16}$$

where v_4 — the initial velocity at which the runaway vehicle and the baffle wall start to move together in m/s, M— the total weight of the baffle wall and the hydraulic rod in kg.

The expression of v_4 obtained using Eq. (16) is written in Eq. (17).

$$v_4=\frac{mv_3}{m+M} \tag{17}$$

During the process of a runaway vehicle from speed v_4 to full braking, the forces experienced by it mainly include the air resistance, rolling resistance, gradient resistance, pulling force provided by the cam constant-force mechanism through a steel cable, and other forces.

The calculation formulas of ramp resistance F_{g2}, rolling resistance $F_{\Gamma 2}$, and air resistance F_{a2} are expressed in Eq. (18), (19), and (20), respectively.

$$F_{g2}=\left(m+M\right)g\sin\alpha \tag{18}$$

$$F_{\Gamma 2}=\left(m+M\right)gD_f\text{, and} \tag{19}$$

$$F_{a2}=\frac{\int_0^{v_4}\frac{KA_1\rho V^2}{2}dV}{v_4} \tag{20}$$

Based on the law of conservation of energy, Eq. (21) can be obtained for this process.

$$\frac{1}{2}(m+M)v_4^2=(m+M)g(L-l)\sin\alpha + (F_{\Gamma 2}+F_{a2})(L-l)+W_{f2}+T(L-l) \quad (21)$$

where L — the maximum usable distance of the braking ramp in m and W_{f2} — the total work done by other forces.

The pulling force is obtained using Eq. (21) as shown in Eq. (22).

$$T=\frac{\frac{1}{2}(m+M)v_4^2-W_{f2}}{L-l}-(m+M)g\sin\alpha - F_{\Gamma 2}-F_{a2} \quad (22)$$

5. Simulation Analysis

5.1. Parameter Settings

To verify the effectiveness of the intelligent control model of the escape lane proposed in this paper, this section simulates the whole process of braking the runaway vehicle entering the escape lane. Select light, medium, and heavy trucks as simulation objects, and their masses are set to 4500 kg, 12000 kg, and 30000 kg, respectively. The initial speeds of all vehicles before entering the TER are set between 60 km/h and 120 km/h. After the simulation objects are determined, set other parameters in the model according to the actual situation. The parameter settings of the simulation model are listed in Table 1. In addition, to analyze the influence of t_1 on the system, this study divides the out-of-control vehicle motion simulation into three groups. In the three groups, the values of t_1 are set as 1 s, 2 s, and 3 s, respectively.

5.2. Simulation Results

The mathematical model of the braking process can be converted into a computer simulation model. The mathematical models of a_w and T in section 4 can be converted into computer simulation models by using Matlab/SIMULINK. The simulation models based on SIMULINK are shown in Fig. 8 and 9.

Table 1. Parameter settings in the simulation model

Parameter name	Symbol	Numerical value
Brake ramp angle	α	1.72°
Approach length	L_y	300 m
Coefficient of air resistance	K	0.75
Total weight of baffle wall and hydraulic rod	M	5000 kg
Maximum usable distance of braking ramp	L	300
Windward area of vehicle	A_1	6 m^2
Air density	ρ	1.2258 $N \cdot s^2/m^4$
Rolling resistance coefficient	D_f	0.037
Windward area of vehicle	A_2	6.8 m^2
Total work done by other forces	W_{f1}	0
Total work done by other forces	W_{f2}	0

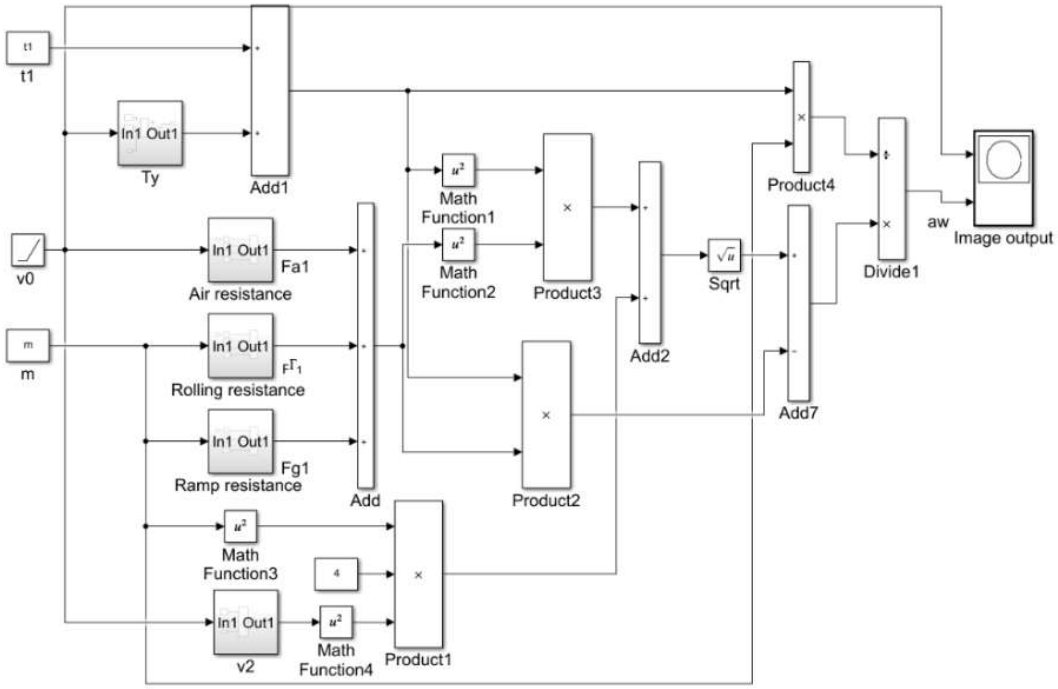

Fig. 8. Establishment of simulation model of a_w

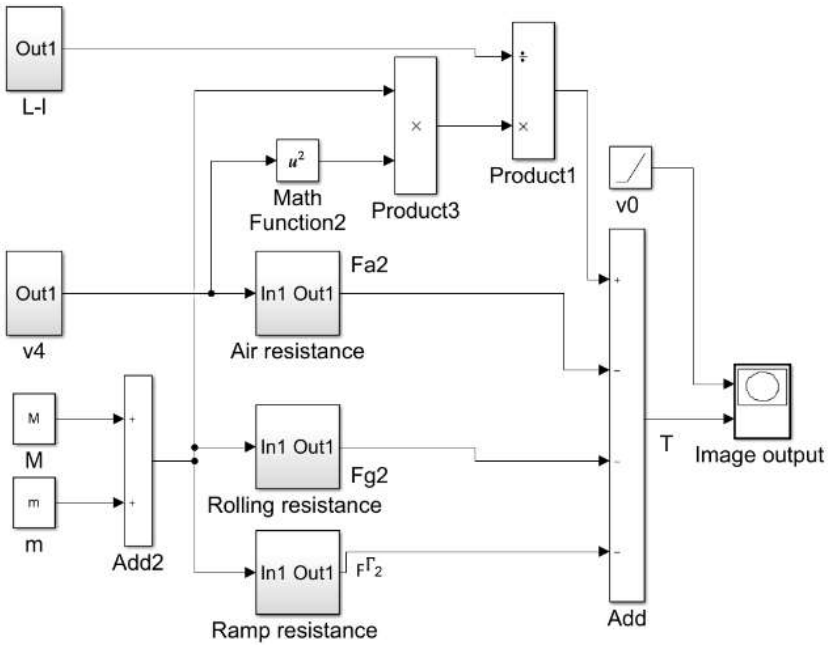

Fig. 9. Establishment of a simulation model of *T*

After the simulation model is established, the relationships between the initial speed of different quality out-of-control vehicles and the acceleration of the baffle wall and the pulling force provided by the cam constant-force mechanism are recorded. The simulation results are shown in Fig. 10, 11, and 12.

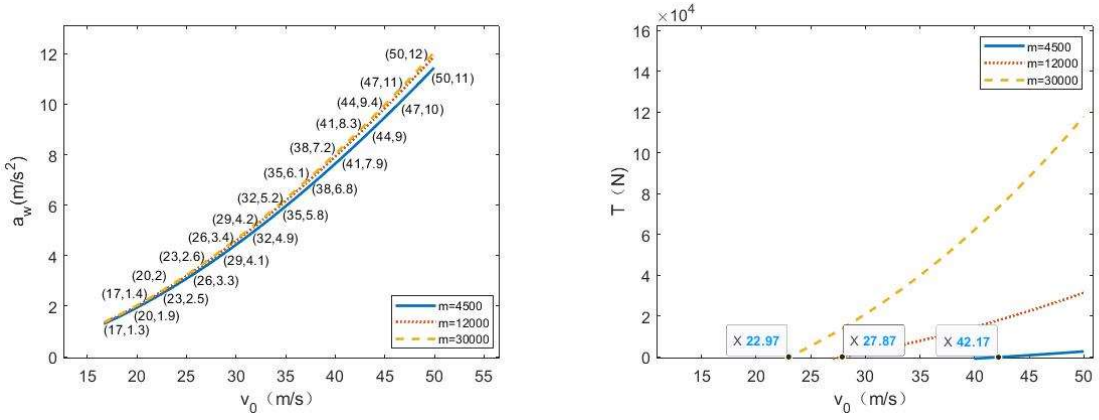

(**a**) (**b**)

Fig. 10. Relationship curve between vehicle initial speed and baffle acceleration (**a**) and pulling force (**b**) for t_1=1 s

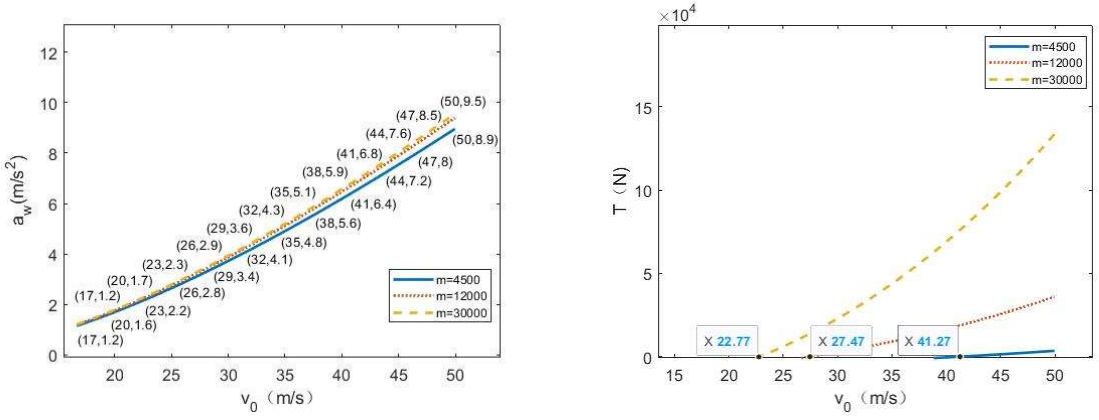

(**a**) (**b**)

Fig. 11. Relationship curve between vehicle initial speed and baffle acceleration (**a**) and pulling force (**b**) for t_1=2 s

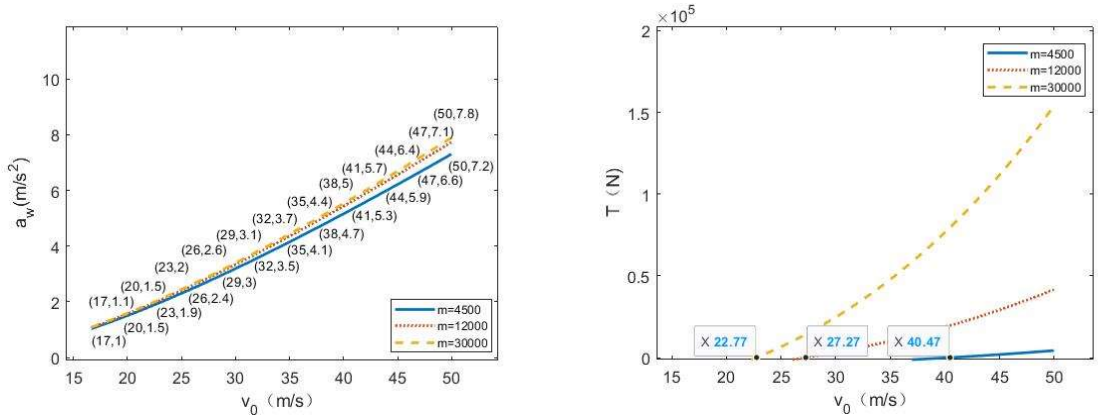

(**a**) (**b**)

Fig. 12. Relationship curve between vehicle initial speed and baffle acceleration (**a**) and pulling force (**b**) for t_1=3 s

Table 2. Simulation results

Index	M = 4500 kg		M = 12000 kg		M = 30000 kg	
	Range of pulling force (N)	Critical velocity (m/s)	Range of pulling force (N)	Critical velocity (m/s)	Range of pulling force (N)	Critical velocity (m/s)
t_1 = 1	0–2713	41.3	0–31100	27.4	0–117700	23.0
t_1 = 2	0–3485	41.2	0–416000	27.5	0–133700	22.8
t_1 = 3	0–4228	40.5	0–133700	27.3	0–152000	22.8

5.3. Result Analysis

According to Figures 10–12, it can be obtained that the acceleration of the baffle wall increases with the increase in the initial speed of the vehicle. Moreover, the mass of the vehicle has a small effect on the acceleration of the baffle wall, whereas the value of t_1 has a certain influence on it. The ranges of the acceleration of the baffle at t_1 = 1, 2, and 3 are 1.3–12.0 m/s^2, 1.2–9.5 m/s^2, and 1.0–7.8 m/s^2, respectively. When the vehicle speed is smaller than and greater than 35 m/s, the influence ranges are approximately 0.5 m/s^2 and approximately 1 ~ 2 m/s^2, respectively.

According to the simulation, the ranges of the pulling force under different conditions and the critical speed of the vehicle at which the pulling force starts can be obtained, as summarized in Table 2. The pulling force is positively correlated with t_1, the vehicle mass, and the speed. The critical speed mainly depends on the vehicle mass, with a high mass implying a low critical speed.

Summarizing, the proposed intelligent control method for a TER has a good safety braking effect under various working conditions. Considering the uncontrollability of an out-of-control vehicle when driving alone, based on the achievable acceleration of the baffle wall, t_1 should be selected to be small to the maximum extent. When the braking system provides the pulling force to exert the braking effect, the mass of the runaway vehicle is negatively correlated with the critical speed. Therefore, for vehicles with small masses, the system mainly functions to stabilize the vehicle and prevent it from deviating or turning over. For high-speed and heavy vehicles, the system mainly exerts its braking control effect on the basis of stabilizing vehicles, ensuring that the runaway vehicles utilize most of the braking ramp length, and preventing secondary injuries.

6. Conclusion

Based on the combination of the theory of momentum theorem and information technology, this paper establishes an intelligent control model for escape lanes to control the running states of runaway vehicles. So as to reduce the external forces during vehicle deceleration and reduce the probability of secondary accidents of out-of-control vehicles. MATLAB/SIMULINK software is used to obtain the simulation data to calibrate and verify the built intelligent control model. The changes in control parameters (acceleration of the baffle wall and pulling force provided by the cam constant-force mechanism) are analyzed under different vehicle masses, vehicle speeds, and operating time conditions. The research results show that under the condition of using a slope aggregate with a small rolling resistance coefficient, the intelligent control method can ensure that a runaway vehicle fully utilizes the braking ramp to complete braking. For the safety braking of high-speed and heavy-duty vehicles, the system can provide full use of its role. Therefore, the intelligent control method of the escape lane proposed in this paper can be used by the highway administration to redesign the braking device, the length of the ramp, and the slope aggregate.

The intelligent control method for an escape lane proposed in this study ignores other interference factors including the accuracy of the measuring equipment, friction between the car and the baffle wall, friction between the hydraulic rod and the track, and other forces on the system. In the future, the key factors that affect the accuracy of the model will be discussed and improved to increase the control accuracy. In addition, this study did not conduct an in-depth investigation on the lateral movement of the baffle wall and the process of fitting with the runaway vehicle, which is one of the basic directions of the follow-up research.

References

Al-Madani, H. and Al-Janahi, A. R. (2002). Assessment of drivers' comprehension of traffic signs based on their traffic, personal and social characteristics. *Transportation research part F: Traffic psychology and behaviour*, 5(1), 63-76. doi: 10.1016/S1369-8478(02)00006-2

Bauskar, M. P., Dhande, D. Y., Vadgeri, S., and Patil, S. (2019). Study of aerodynamic drag of sports utility vehicle by experimental and numerical method. *Materials Today: Proceedings*, 16, 750-757. doi: 10.1016/j.matpr.2019.05.155

Capuano, F. A., Heymsfield, E., and Li, N. (2018). Alternative arresting system design for truck escape ramps. *International journal of crashworthiness*, 23(6), 618-626. doi: 10.1080/13588265.2017.1368120

Greto, K. and Easa, S. M. (2019). Reliability-based design of truck escape ramps. *Canadian Journal of Civil Engineering*, 47(4), 395-404. doi: 10.1139/cjce-2018-0720

Hancock, M. W. and Wright, B. (2013). *A policy on geometric design of highways and streets*. Washington, DC, USA: American Association of State Highway and Transportation Officials, 1-13.

Haugland, O. A. (2013). Walking through the impulse-momentum theorem. *The Physics Teacher*, 51(2), 78-79. doi: 10.1119/1.4775522

Mi, X., Jia, N., and Wan, J. (2020). Design and safety considerations for highway safety facilities of truck escape ramp. *Highway*, 65(4), 243. doi: 10.12159/j.issn.2095-6630.2020.31.1519

Michael, M., Vogel, F., and Peters, B. (2015). DEM–FEM coupling simulations of the interactions between a tire tread and granular terrain. *Computer Methods in Applied Mechanics and Engineering*, 289, 227-248. doi: 10.1016/j.cma.2015.02.014

Nishiyama, K., Nakashima, H., Shimizu, H., Miyasaka, J., and Ohdoi, K. (2017). 2D FE–DEM analysis of contact stress and tractive performance of a tire driven on dry sand. *Journal of Terramechanics*, 74, 25-33. doi: 10.1016/j.jterra.2017.09.003

Patole, S. M., Torlak, M., Wang, D., and Ali, M. (2017). Automotive radars: A review of signal processing techniques. *IEEE Signal Processing Magazine*, 34(2), 22-35. doi: 10.1109/MSP.2016.2628914

Pawłowicz, B., Trybus, B., Salach, M., and Jankowski-Mihułowicz, P. (2020). Dynamic RFID identification in urban traffic management systems. *Sensors*, 20(15), 4225. doi: 10.3390/s20154225

Qin, P., Hou, X., Zhang, S., and Wu, D. (2021). Design and simulation of flexible safety net applied in truck escape ramp. *China Sciencepaper*, 16(06), 578-584. doi: 10.3969/j.issn.2095-2783.2021.06.002

Raslavičius, L., Keršys, A., and Makaras, R. (2017). Management of hybrid powertrain dynamics and energy consumption for 2WD, 4WD, and HMMWV vehicles. *Renewable and Sustainable Energy Reviews*, 68, 380-396. doi: 10.1016/j.rser.2016.09.109

Shariff, K. K. M., Hoare, E., Daniel, L., Antoniou, M., and Cherniakov, M. (2017). Comparison of adaptive spectral estimation for vehicle speed measurement with radar sensors. *Sensors*, 17(4), 751. doi: 10.3390/s17040751

Song, C. and Guo, Z. (2017). Width of cross section on truck escape ramp based on driving simulation. *Journal of Tongji University (Natural Science)*, 45(1), 46-52. doi: 10.11908/j.issn.0253-374x.2017.01.007

Song, C., Guo Z., and Lin, Z. (2016). Departure angle and approach length of truck escape ramp. *Journal of Tongji University*, 44(4), 587-592. doi: 10.11908/j.issn.0253-374x.2016.04.013

Song, C., Guo Z., and Song, C. (2016). Location of full-width service lanes on truck escape ramp. *Journal of Tongji University (Natural Science)*, 44(10), 1559-1566. doi: 10.11908/j.issn.0253-374x.2016.10.013

Wang, W. and Zhang, Z. (2012). Design of emergency escaping lane of mountainous highway. *Highway Engineering*, 37(1), 107-110. doi: 10.3969/j.issn.1674-0610.2012.01.026

Wu, J. (2006). Layout of truck escape ramp on mountain highways. *Highway*, 7, 105-109. doi: 10.3969/j.issn.0451-0712.2006.07.026

Yan, S., Fang, L., Ma, L., and Jin, K. (2015). Net energy absorption system for a truck escape ramp. *Journal of Vibration and Shock*, 34(17), 30-37. doi: 10.13465/j.cnki.jvs.2015.17.006

Zhao, J., Xu, H., Liu, H., Wu, J., Zheng, Y., and Wu, D. (2019). Detection and tracking of pedestrians and vehicles using roadside LiDAR sensors. *Transportation research part C: emerging technologies*, 100, 68-87. doi: 10.1016/j.trc.2019.01.007

Xinghua Hu was born in China, in 1981. He received the Ph. D. degree from Beijing Jiaotong University, in 2016. His current research interests include Urban and regional transportation planning, green transportation, intelligent transportation. He is currently a professor of Chongqing Jiaotong University, deputy director of Chongqing Key Laboratory of transportation engineering, green transportation expert of the Ministry of transportation and Chongqing comprehensive bid evaluation expert. From 2016 to 2021, he presided over and participated in more than 10 national, provincial and ministerial scientific research projects, presided over and participated in the preparation of 11 national transportation industry energy conservation and emission reduction project guidelines, local industry standards and so on. Published more than 30 papers and 6 monographs, and won 5 provincial and ministerial awards such as Chongqing Development Research Award, Chongqing Social Science Outstanding Achievement Award, and China Highway Society Science and Technology Award.

Hongbin Qin was born in Chongqing, China, in 1996. He received the B. E. degree from the School of Traffic and Transportation, Chongqing Jiaotong University, in 2018, where he is currently pursuing a master's degree. His current research interests include green energy transportation and transportation planning and management.

Yaqi Zhu was born in Chongqing, China. He received the B. E. degree from the School of Traffic and Transportation, Chongqing Jiaotong University, in 2021, where he is currently pursuing the master's degree. His current research interests include transportation planning and management.

Wei Liu was born in China, in 1978. He received the Ph.D. degree from Southwest Jiaotong University, in 2011. His current research interests include traffic system planning and intelligent management, road traffic safety and improvement design and other fields. He is currently a professor of Chongqing Jiaotong University, director of the Institute of transportation engineering, School of transportation, Chongqing Jiaotong University, chairman of the Technical Committee for traffic organization and operation management of the Transportation Engineering Department of the world transportation Congress, director of China Society of transportation engineering, expert of China Road Traffic safety think tank, vice president and Secretary General of Chongqing safety production accident research association Deputy Secretary General of urban transportation special committee of Chongqing Planning Society, expert of Chongqing automatic driving on the road expert committee, expert of Chongqing vehicle management expert advisory committee, and expert of Chongqing Comprehensive Transportation Planning Advisory Committee. From 2011 to 2021, his scientific research projects and achievements have mainly completed more than 110 scientific research projects, won the third prize of provincial and ministerial scientific research progress twice, and the third prize of social development research award. He has guided students to win the National University Student Transportation Science and Technology Competition twice. , Completed 3 innovation and entrepreneurship training projects, instructed students to apply for 1 invention patent and 2 utility model invention patents, published more than 30 papers.

Gao Dai was born in China, in 1966. He received the master degree from Huazhong University of Science and Technology, 1989. He is currently the general manager of Chongqing Ulit Science & Technology Co., Ltd. His current research interests include traffic behavior and big data modeling application, intelligent traffic control, construction of road traffic facilities.